Applications of Mathematics

Jiří Krček
BIE model of periodic diffraction problems in optics

Applications of Mathematics, Vol. 67 (2022), No. 1, 81–92

Persistent URL: `http://dml.cz/dmlcz/149360`

67 (2022) APPLICATIONS OF MATHEMATICS No. 1, 81–92

BIE MODEL OF PERIODIC DIFFRACTION PROBLEMS IN OPTICS

Jiří Krček, Ostrava

Received April 7, 2020. Published online August 13, 2021.

Abstract. Optical diffraction on a periodical interface belongs to relatively lowly exploited applications of the boundary integral equations method. This contribution presents a less frequent approach to the diffraction problem based on vector tangential fields of electromagnetic intensities. The problem is formulated as the system of boundary integral equations for tangential fields, for which existence and uniqueness of weak solution is proved. The properties of introduced boundary operators with singular kernel are discussed with regard to performed numerical implementation. Presented theoretical model is of advantage when the electromagnetic field near the material interface is studied, that is illustrated by several application outputs.

Keywords: optical diffraction; tangential fields; boundary elements method

MSC 2020: 78A45, 45P05

1. Introduction

The diffraction of an optical wave on a periodical interface between two media belongs to frequently solved problems, especially when the grating period Λ is comparable with the wavelength of the incident beam. Among other, these phenomena are studied and exploited for nanostructured optical devices design as nanosensors or integrated optics elements ([7], [8]). Naturally, the theoretical modelling is of great importance in such cases. During the last thirty years, numerous works treating the optical diffraction in periodical structures have been published (see [1]) and references therein. One of the relatively new approaches is based on the Boundary Integral Equations (BIE) [2], [5]. In this article, we present specific integral formulation of the boundary problem for the system of the Maxwell equations based on the tangential vector fields and propose its numerical implementation.

In comparison with the usually used rigorous coupled waves algorithm (RCWA) [11], [13] that is advantageous especially in the far fields analysis, the BIE models

DOI: 10.21136/AM.2021.0098-20

enable effective modelling of near fields in the spatially modulated region. But modelling of far fields by BIE models is possible too if need be. Other advantage of BIE models is their applicability to problems where the height of the interface profile is comparable with its period, whereas the RCWA models do not work satisfactorily in such cases. Similar and often used way of modelling of diffraction problems is the Finite-Difference Time-Domain (FDTD) technique [15]. Unlike the presented model based on tangential fields of electromagnetic intensity vectors, the FDTD method is working directly with intensity vectors components.

2. Formulation of problem

We study the optical diffraction problem on a smooth interface S between two homogeneous materials. Let $S\colon\ x_3 = f(x_1)$ in $\mathbb{R}^3$ be a smooth surface periodically modulated in the coordinate x_1 with the period Λ and uniform in the x_2 direction. The periodical interface S with the unit normal vector $\boldsymbol{\nu}$ divides the space into two semi-infinite homogeneous domains $\Omega^{(1)}$ and $\Omega^{(2)}$, where the materials are characterized by the constant relative permittivities $\varepsilon^{(1)} \neq \varepsilon^{(2)}$, $\varepsilon^{(1)} \in \mathbb{R}$ and $\varepsilon^{(2)} \in \mathbb{C}$, $\mathrm{Re}\,(\varepsilon^{(2)}) > 0$, $\mathrm{Im}\,(\varepsilon^{(2)}) \geqslant 0$ and the relative permeabilities $\mu^{(1)} = \mu^{(2)} = 1$ (both the materials are supposed to be magnetically neutral), see Figure 1.

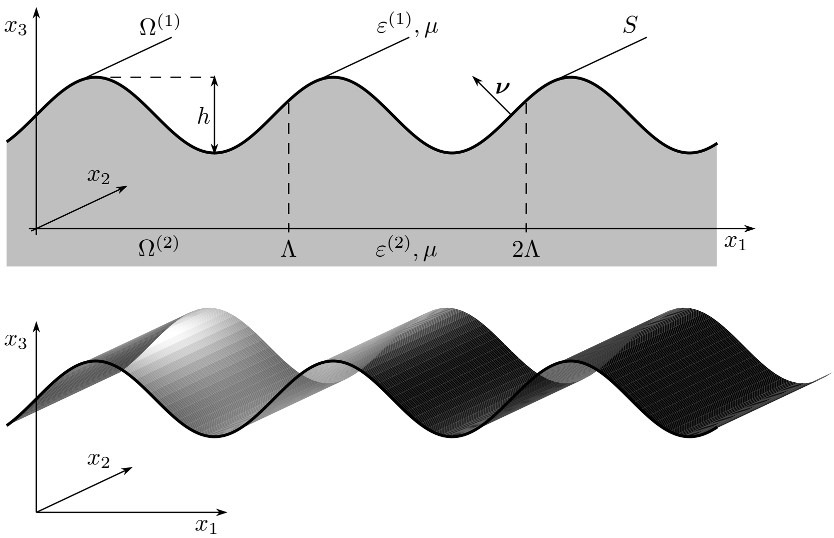

Figure 1. Semi-infinite domains with common periodical boundary.

We aim to solve the optical diffraction problem for an incident monochromatic plane wave with the wavelength λ, corresponding free-space wave number $k_0 = 2\pi/\lambda$

and the wave vector $\boldsymbol{k} = (\alpha, 0, \beta)$, that is incoming from the domain $\Omega^{(1)}$ under the incidence angle θ measured from the x_3 direction. We seek for the space-dependent amplitudes $\boldsymbol{E}^{(j)} = \boldsymbol{E}|_{\Omega^{(j)}}$, $\boldsymbol{H}^{(j)} = \boldsymbol{H}|_{\Omega^{(j)}}$ of the electromagnetic field intensity vectors $\boldsymbol{E}(x_1, x_2, x_3)\mathrm{e}^{-\mathrm{i}\omega t}$, $\boldsymbol{H}(x_1, x_2, x_3)\mathrm{e}^{-\mathrm{i}\omega t}$, where $\omega = c/\lambda$ and c represents the speed of light in the free-space. The unknown intensities can be written as (the subscript 0 denotes the incident field)

$$\boldsymbol{E} = \begin{cases} \boldsymbol{E}_0^{(1)} + \boldsymbol{E}^{(1)} & \text{in } \Omega^{(1)}, \\ \boldsymbol{E}^{(2)} & \text{in } \Omega^{(2)}, \end{cases} \qquad \boldsymbol{H} = \begin{cases} \boldsymbol{H}_0^{(1)} + \boldsymbol{H}^{(1)} & \text{in } \Omega^{(1)}, \\ \boldsymbol{H}^{(2)} & \text{in } \Omega^{(2)}. \end{cases} \tag{2.1}$$

In the media without free charges, the vectors $\boldsymbol{E}^{(j)}$, $\boldsymbol{H}^{(j)}$, $j = 1, 2$, fulfil the Maxwell equations

$$\nabla \times \boldsymbol{E}^{(j)} = \mathrm{i}k_0\mu\boldsymbol{H}^{(j)}, \quad \nabla \times \boldsymbol{H}^{(j)} = -\mathrm{i}k_0\varepsilon^{(j)}\boldsymbol{E}^{(j)} \quad \text{in } \Omega^{(j)}, \tag{2.2}$$

$$\nabla \cdot \boldsymbol{E}^{(j)} = 0, \quad \nabla \cdot \boldsymbol{H}^{(j)} = 0 \quad \text{in } \Omega^{(j)}, \tag{2.3}$$

where the free space impedance $\sqrt{\mu_0/\varepsilon_0}$ is without loss of generality included in the vector $\boldsymbol{H}$. The tangential components are continuous on the boundary

$$\boldsymbol{\nu} \times (\boldsymbol{E}^{(1)} - \boldsymbol{E}^{(2)}) = \boldsymbol{o}, \quad \boldsymbol{\nu} \times (\boldsymbol{H}^{(1)} - \boldsymbol{H}^{(2)}) = \boldsymbol{o} \quad \text{on } S, \tag{2.4}$$

where $\boldsymbol{o} = (0, 0, 0)$ is the zero vector.

For the far fields, the well-known Sommerfeld radiation convergence conditions at infinity hold which enables to consider the problem on the common interface S only [9]. With respect to studied plasmonic applications we solve problem (2.2)–(2.4) for the transverse magnetic (TM) polarization of the incident wave, for which

$$\boldsymbol{E}^{(j)} = (E_1^{(j)}, 0, E_3^{(j)}), \quad \boldsymbol{H}^{(j)} = (0, H_2^{(j)}, 0). \tag{2.5}$$

The Maxwell equations (2.2), (2.3) lead to the Helmholtz equations for the scalar components $H_2^{(j)}$,

$$\Delta H_2^{(j)} + k_0^2\varepsilon^{(j)}H_2^{(j)} = 0 \quad \text{on } \Omega^{(j)}, \quad j = 1, 2. \tag{2.6}$$

Denoting $\boldsymbol{x} = (x_1, x_3)$, $\boldsymbol{y} = (y_1, y_3)$, the periodical fundamental solution of the Helmholtz equation in $\Omega^{(j)}$ can be written as [12]

$$\begin{aligned} \Psi^{(j)}(\boldsymbol{x}, \boldsymbol{y}) &= \frac{1}{2\mathrm{i}\Lambda} \sum_{m=-\infty}^{\infty} \Psi_m^{(j)}(\boldsymbol{x}, \boldsymbol{y}), \\ \Psi_m^{(j)}(\boldsymbol{x}, \boldsymbol{y}) &= \frac{1}{\beta_m^{(j)}} \mathrm{e}^{\mathrm{i}(\alpha_m(x_1 - y_1) + \beta_m^{(j)}|x_3 - y_3|)}, \end{aligned} \tag{2.7}$$

where α_m, $\beta_m^{(j)}$ are the propagation constants introduced as

$$\alpha_m = \alpha + 2\pi m/\Lambda, \quad \alpha = k_0\sqrt{\varepsilon^{(1)}}\sin\theta, \quad \alpha_m^2 + (\beta_m^{(j)})^2 = k_0^2\varepsilon^{(j)}. \tag{2.8}$$

The following theorem introduces an important property of the functions $\Psi^{(j)}$ that we proved in [16].

Theorem 2.1. *For the both functions* $\Psi^{(j)}(\boldsymbol{x},\boldsymbol{y})$ *defined by* (2.7) *and for an arbitrary but fixed* $\boldsymbol{x} \in \mathbb{R}^2$ *the difference*

$$\widetilde{\Psi}^{(j)}(\boldsymbol{y}) = \Psi^{(j)}(\boldsymbol{x},\boldsymbol{y}) - \frac{1}{2\pi}\ln\frac{1}{k\|\boldsymbol{x}-\boldsymbol{y}\|} \tag{2.9}$$

is continuous in $\mathbb{R}^2$.

3. Mathematical model

We formulate the problem (2.2)–(2.4) as the system of boundary integral equations for the scalar factors J_2, I_τ of the tangential vector fields

$$\boldsymbol{J} = \boldsymbol{\nu}\times\boldsymbol{E}^{(1)} = \boldsymbol{\nu}\times\boldsymbol{E}^{(2)} = -J_2\boldsymbol{e}_2, \quad \boldsymbol{I} = -\boldsymbol{\nu}\times\boldsymbol{H}^{(1)} = -\boldsymbol{\nu}\times\boldsymbol{H}^{(2)} = I_\tau\boldsymbol{\tau}, \tag{3.1}$$

where $\boldsymbol{\tau}$ is the unit tangential vector of the boundary S, $J_2 = \boldsymbol{\tau}\cdot\boldsymbol{E}^{(1)} = \boldsymbol{\tau}\cdot\boldsymbol{E}^{(2)}$, $I_\tau = -H_2^{(1)} = -H_2^{(2)}$ and $\boldsymbol{e}_2 = (0,1,0)$, see Figure 2.

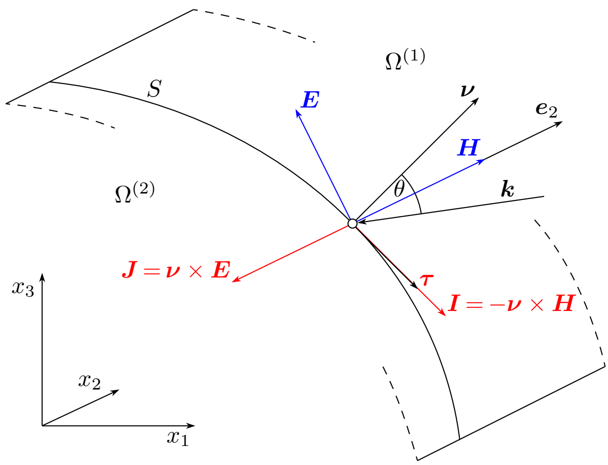

Figure 2. Tangential fields.

Due to periodicity we can reduce the integral formulation only to one period of the boundary. Considering fictitious boundaries $x_1 = 0$ and $x_1 = \Lambda$ we can restrict the problem to domains

$$\Omega^{(1)} = \{\boldsymbol{x}\in\mathbb{R}^2,\ x_1\in(0,\Lambda),\ x_3 > f(x_1)\}, \tag{3.2}$$

$$\Omega^{(2)} = \{\boldsymbol{x}\in\mathbb{R}^2,\ x_1\in(0,\Lambda),\ x_3 < f(x_1)\} \tag{3.3}$$

with common boundary

$$S_\Lambda = \{\boldsymbol{x} \in \mathbb{R}^2,\ x_1 \in [0,\Lambda],\ x_3 = f(x_1)\}. \tag{3.4}$$

Let us note that integrals on newly established fictitious boundaries differ only in signs as a result of periodicity and hence negate each other.

The up till now gained theoretical results are summarized in Theorem 3.1 below. The governing formulas (3.10), (3.11) are based on the theoretical background established in [6], where the constitutional idea of tangential fields on periodic structures was introduced. The fundamental steps and the theoretical statements required to derive these formulas can be found in our article [10].

Other important question not mentioned in the above listed sources and being crucial for the weak formulation is the choice of function spaces. Hence, we establish Sobolev spaces of vector functions with generalized curl on unbounded domains $\Omega^{(j)}$, $j = 1, 2$,

$$\mathsf{H}_{\mathrm{loc}}(\mathbf{curl}, \Omega^{(j)}) = \{\boldsymbol{v} \in \mathbf{L}^2(\overline{\Omega^{(j)}}), \nabla \times \boldsymbol{v} \in \mathbf{L}^2(\overline{\Omega^{(j)}})\} \tag{3.5}$$

that seem to be the most suitable for a weak formulation of Maxwell equations [3]. Further, we denote by $\gamma_0^{(j)}$ the Dirichlet trace of functions from $\mathsf{H}_{\mathrm{loc}}(\mathbf{curl}, \Omega^{(j)})$ on the common boundary S_Λ,

$$\gamma_0^{(j)}:\ \mathsf{H}_{\mathrm{loc}}(\mathbf{curl}, \Omega^{(j)}) \to \mathsf{H}^{1/2}(S_\Lambda). \tag{3.6}$$

The tangential trace of functions $\boldsymbol{v} \in \mathbf{C}^\infty(\overline{\Omega^{(j)}})$ on S_Λ is the mapping

$$\gamma_\tau^{(j)}:\ \boldsymbol{v} \to \boldsymbol{\nu} \times \boldsymbol{v}|_{S_\Lambda} \tag{3.7}$$

that can be continuously extended to the whole space $\mathsf{H}_{\mathrm{loc}}(\mathbf{curl}, \Omega^{(j)})$, and

$$\gamma_\tau^{(j)}:\ \mathsf{H}_{\mathrm{loc}}(\mathbf{curl}, \Omega^{(j)}) \to \mathsf{H}^{-1/2}(\mathrm{div}, S_\Lambda), \tag{3.8}$$

where

$$\mathsf{H}^{-1/2}(\mathrm{div}, S_\Lambda) = \{\boldsymbol{v} \in \mathsf{H}^{-1/2}(S_\Lambda), \mathrm{div}\, \boldsymbol{v} \in \mathrm{H}^{-1/2}(S_\Lambda)\} \tag{3.9}$$

is the space of tangential traces with generalized divergence [4]. The symbols $\mathrm{H}^{-1/2}(S_\Lambda)$ and $\mathsf{H}^{-1/2}(S_\Lambda)$ denote dual spaces to scalar and vector spaces of Dirichlet traces $\mathrm{H}^{1/2}(S_\Lambda)$ and $\mathsf{H}^{1/2}(S_\Lambda)$ (see [14], for instance).

Theorem 3.1. *The intensity vectors* $\boldsymbol{E}^{(j)}$, $\boldsymbol{H}^{(j)} \in \mathsf{H}_{\mathrm{loc}}(\mathbf{curl}, \Omega^{(j)})$, $j = 1, 2$, *defined as*

$$\begin{aligned}(3.10)\quad \boldsymbol{E}^{(j)}(\boldsymbol{x}) &= \mathrm{i}k_0\mu \int_{S_\Lambda} \boldsymbol{I}(\boldsymbol{\eta})\Psi^{(j)}(\boldsymbol{x},\boldsymbol{\eta})\,\mathrm{d}l_\eta + \frac{1}{\mathrm{i}k_0\varepsilon^{(j)}}\nabla_x \int_{S_\Lambda} \boldsymbol{I}(\boldsymbol{\eta})\cdot\nabla_\eta\Psi^{(j)}(\boldsymbol{x},\boldsymbol{\eta})\,\mathrm{d}l_\eta \\ &\quad - \int_{S_\Lambda} \boldsymbol{J}(\boldsymbol{\eta})\times\nabla_\eta\Psi^{(j)}(\boldsymbol{x},\boldsymbol{\eta})\,\mathrm{d}l_\eta,\\ (3.11)\quad \boldsymbol{H}^{(j)}(\boldsymbol{x}) &= \mathrm{i}k_0\varepsilon^{(j)} \int_{S_\Lambda} \boldsymbol{J}(\boldsymbol{\eta})\Psi^{(j)}(\boldsymbol{x},\boldsymbol{\eta})\,\mathrm{d}l_\eta + \frac{1}{\mathrm{i}k_0\mu}\nabla_x \int_{S_\Lambda} \boldsymbol{J}(\boldsymbol{\eta})\cdot\nabla_\eta\Psi^{(j)}(\boldsymbol{x},\boldsymbol{\eta})\,\mathrm{d}l_\eta \\ &\quad + \int_{S_\Lambda} \boldsymbol{I}(\boldsymbol{\eta})\times\nabla_\eta\Psi^{(j)}(\boldsymbol{x},\boldsymbol{\eta})\,\mathrm{d}l_\eta,\end{aligned}$$

represent the unique weak solution of problem (2.2)–(2.4), *even as the scalar factors* J_2, $I_\tau \in \mathsf{H}^{-1/2}(S_\Lambda)$ *of the vector tangential fields* $\boldsymbol{I}$, $\boldsymbol{J} \in \mathbf{H}^{-1/2}(\mathrm{div}, S_\Lambda)$, $\boldsymbol{J} = -J_2\boldsymbol{e}_2$, $\boldsymbol{I} = I_\tau\boldsymbol{\tau}$, *fulfil the system of integral equations*

$$\begin{aligned}(3.12)\quad & -\mathrm{i}k_0\mu\boldsymbol{\tau}_\xi\cdot\int_{S_\Lambda} I_\tau(\boldsymbol{\eta})\boldsymbol{\tau}_\eta(\Psi^{(1)}(\boldsymbol{\xi},\boldsymbol{\eta}) - \Psi^{(2)}(\boldsymbol{\xi},\boldsymbol{\eta}))\,\mathrm{d}l_\eta \\ &\quad - \frac{1}{\mathrm{i}k_0}\boldsymbol{\tau}_\xi\cdot\int_{S_\Lambda} \varrho I_\tau(\boldsymbol{\eta})\nabla_\eta\Big(\frac{1}{\varepsilon^{(1)}}\Psi^{(1)}(\boldsymbol{\xi},\boldsymbol{\eta}) - \frac{1}{\varepsilon^{(2)}}\Psi^{(2)}(\boldsymbol{\xi},\boldsymbol{\eta})\Big)\,\mathrm{d}l_\eta \\ &\quad + J_2(\boldsymbol{\xi}) - \boldsymbol{\nu}_\xi\cdot\int_{S_\Lambda} J_2(\boldsymbol{\eta})\nabla_\eta(\Psi^{(1)}(\boldsymbol{\xi},\boldsymbol{\eta}) - \Psi^{(2)}(\boldsymbol{\xi},\boldsymbol{\eta}))\,\mathrm{d}l_\eta = -J_{2,0}(\boldsymbol{\xi}),\\ (3.13)\quad & I_\tau(\boldsymbol{\xi}) + \mathrm{i}k_0\int_{S_\Lambda} J_2(\boldsymbol{\eta})(\varepsilon^{(1)}\Psi^{(1)}(\boldsymbol{\xi},\boldsymbol{\eta}) - \varepsilon^{(2)}\Psi^{(2)}(\boldsymbol{\xi},\boldsymbol{\eta}))\,\mathrm{d}l_\eta \\ &\quad - \int_{S_\Lambda} I_\tau(\boldsymbol{\eta})\boldsymbol{\nu}_\eta\cdot\nabla_\eta(\Psi^{(1)}(\boldsymbol{\xi},\boldsymbol{\eta}) - \Psi^{(2)}(\boldsymbol{\xi},\boldsymbol{\eta}))\,\mathrm{d}l_\eta = -I_{\tau,0}(\boldsymbol{\xi}),\end{aligned}$$

where

$$(3.14)\qquad J_{2,0}(\boldsymbol{\xi}) = \boldsymbol{\tau}_\xi\cdot\boldsymbol{E}_0^{(1)}(\boldsymbol{\xi}),\quad I_{\tau,0}(\boldsymbol{\xi}) = -H_{0,2}^{(1)}(\boldsymbol{\xi}).$$

P r o o f. The applicability of function spaces used in the weak formulation above to the problems related to the Maxwell equations was presented in [3], where the existence and uniqueness of the weak solution of the primary problem (2.2)–(2.4) were proved in a general case.

The equivalence of problems (3.10), (3.11) and (3.12), (3.13) results from the relations between the tangential fields and the intensity vectors derived in [10], whereas these relations remain in force even on established function spaces under authority of properties of these spaces and of applied differential operators, that were proved in [3] and [4].

The existence and the uniqueness of weak solution of problem (3.12), (3.13) can be verified using the Fredholm alternative (see [14], for instance). In article [6], the compactness of integral operators of the same type as those in the formulas above has been proved. The relevant homogeneous problem corresponds to the incident wave of zero intensity that evidently produces only trivial solution of this problem. □

In relation to numerical implementation we introduce a suitable parametrization $\boldsymbol{\pi}\colon \mathbb{R} \to \mathbb{R}^2$, $\boldsymbol{\pi}(t) = (p(t), q(t))$ of the boundary S such that its one period S_Λ (cf. (3.4)) corresponds to $t \in [0, 2\pi]$. We denote by $\boldsymbol{\nu}(t)$ the normal vector to S and by $\nu(t)$ its magnitude.

The system of integral equations (3.12), (3.13) can be introduced in the operator form ($\mathcal{I}$ is the identity operator)

$$\begin{bmatrix} \mathcal{V}_1 + \mathcal{V}_2 & \mathcal{I} - \mathcal{V}_3 \\ \mathcal{I} - \mathcal{V}_4 & \mathcal{V}_5 \end{bmatrix} \begin{bmatrix} I_\tau \\ J_2 \end{bmatrix} = \begin{bmatrix} -J_{2,0} \\ -I_{\tau,0} \end{bmatrix}. \tag{3.15}$$

Let us emphasize an important fact that the operators $\mathcal{V}_l$, $l = 1, \ldots, 5$, can be rewritten and generally presented as (multiplication constants are omitted for simplification)

$$(\mathcal{V}_l u)(s) = \int_0^{2\pi} u(t)(c_1\Psi^{(1)}(s,t) - c_2\Psi^{(2)}(s,t))\nu(t)\,\mathrm{d}t, \tag{3.16}$$

where $\Psi^{(1)}(s,t)$, $\Psi^{(2)}(s,t)$ are parametrized Green functions (2.7), c_1, c_2 are generally different complex constants and u represents one of the parametrized scalar factors I_τ or J_2.

Theorem 3.2. *Let $\Psi^{(j)}(s,t)$, $j = 1, 2$, be the parametrized Green functions defined by* (2.7) *and $c_1, c_2 \in \mathbb{C}$. Then the differences $c_1\Psi^{(1)}(s,t) - c_2\Psi^{(2)}(s,t)$ are continuous in $\mathbb{R} \times \mathbb{R}$ for $c_1 = c_2$ and have the singularity of the logarithmic type for $c_1 \neq c_2$.*

P r o o f. The considered differences are evidently continuous for $s \neq t$, whereas the singular case occurs for $s = t$ and must be enquired separately. The mth term b_m of the difference series is

$$b_m = \frac{\mathrm{i}}{2\Lambda}\Big(\frac{c_1}{\beta_m^{(1)}} - \frac{c_2}{\beta_m^{(2)}}\Big) = \frac{1}{4\pi}\frac{c_1B_2 - c_2B_1}{B_1B_2}, \tag{3.17}$$

where

$$B_j = \frac{\mathrm{i}\Lambda}{2\pi}\beta_m^{(j)} = \sqrt{\Big(m + \frac{\Lambda}{\lambda}\sqrt{\varepsilon^{(1)}}\sin\theta\Big)^2 - \Big(\frac{\Lambda}{\lambda}\Big)^2\varepsilon^{(j)}}, \quad j = 1, 2. \tag{3.18}$$

The degree of the term b_m is -1 for $c_1 \neq c_2$ and that is why the sum of the series has a weak singularity in this case. If $c_1 = c_2 = c$, then (3.17) can be converted to the form

$$b_m = \frac{c}{4\pi}\left(\frac{\Lambda}{\lambda}\right)^2 \frac{\varepsilon^{(1)} - \varepsilon^{(2)}}{B_1 B_2 (B_2 + B_1)}, \tag{3.19}$$

that is of degree -3 and the series is absolutely convergent. □

Singularity of the logarithmic type is of the key importance, because together with the statement

$$\ln \frac{1}{k\|\boldsymbol{\pi}(s) - \boldsymbol{\pi}(t)\|} = \sum_{\substack{m\in\mathbb{Z}\\ m\neq 0}} \frac{\mathrm{e}^{-\mathrm{i}m(s-t)}}{2k|m|} \tag{3.20}$$

that we proved in [16] and with Theorem 2.1 it enables to split the operators into the compact ones with the continuous kernels and the other with the logarithmic singularity according to the following notation:

$$\Psi^{(j)}(s,t) = \Psi_r^{(j)}(s,t) + \psi(s,t). \tag{3.21}$$

Here we write

$$\Psi_r^{(j)}(s,t) = \Psi_0^{(j)}(s,t) + \sum_{\substack{m\in\mathbb{Z}\\ m\neq 0}} \left(\Psi_m^{(j)}(s,t) - \frac{1}{2\pi}\frac{\mathrm{e}^{-\mathrm{i}m(s-t)}}{2k|m|}\right) \tag{3.22}$$

for the regular part and

$$\psi(s,t) = \frac{1}{2\pi} \sum_{\substack{m\in\mathbb{Z}\\ m\neq 0}} \frac{\mathrm{e}^{-\mathrm{i}m(s-t)}}{2k|m|} \tag{3.23}$$

for the singular one.

4. Numerical implementation

To solve the system of boundary integral equations (3.12), (3.13) we use collocation method with equidistant collocation points. The choice of the appropriate basis functions system appears to be very important. After experiments with usually used systems of linear or cubic splines we prefer the system of trigonometric polynomials with the nodes identical to collocation points, because the structure of trigonometric polynomials is analogous to the structure of singular parts (3.23) of Green functions (2.7) in the integral operators kernels.

With respect to character of input data, the accuracy of numerical calculations is given by number of collocation points as well as by number of used diffraction orders, whereas the influences of both these quantities to output accuracy is assumed to be in correlation, as we verified by experimental calculations. Therefore, we find advantageous to take the order of the boundary discretization equal to the order of the diffraction modes truncation of Green functions.

Since the integral operators in solved system can be split in accordance with (3.21), we evaluate numerically the compact operators with the continuous kernels equivalent to (3.22)—the trapezoidal rule with the nodes in the collocation points gives sufficiently accurate results. The logarithmic-type singular operators with kernels equivalent to (3.23) are computed analytically whereas due to using the trigonometric basis we are to integrate only exponential functions. Application of bases of linear (or cubic) splines appears quite disadvantageous now, because then we would be to integrate products of linear (or cubic) polynomials and exponential functions. The resulting formulas would be more complicated in such cases.

Obtained discrete solution of system (3.15) represents values of scalar factors I_τ and J_2 at collocation points. The representation formulas (3.10), (3.11) then enable us to calculate values of components of the electromagnetic intensity vectors $\boldsymbol{E}$ and $\boldsymbol{H}$ at arbitrary far points in the space that are usually required in many practical applications.

5. Numerical results

To test the presented mathematical model we consider the smooth sine interface $S\colon\ x_3 = \frac{1}{2}h(1+\cos(2\pi x_1/\Lambda))$, $x_1 \in [0,\Lambda]$, $\Lambda = 500$ nm, $h = 50$ nm.

In the following examples, the electromagnetic field near the interface between two dielectrics (air $n_1 = 1$, glass $n_2 = 1.5$) and between the dielectric (glass $n_1 = 1.5$) and the metal (gold $n_2 = 0.1838 + 3.43\mathrm{i}$) is modelled. The incident beam of the wavelength $\lambda = 632.8$ nm (red light) propagates under the angle of incidence θ.

Figures 3 and 4 illustrate distribution of absolute value of the tangential (i.e. continuous) component H_2 of the magnetic intensity vector $\boldsymbol{H} = (0, H_2, 0)$ with the normed incident field. Here, the dissimilarity between the diffraction on the non-absorbing and absorbing media is well visible.

The applicability of presented model for two typical material combinations has been sufficiently verified. All numerical outputs were obtained by our own program code in the Matlab software.

6. Applications

The most used quantity in many applications where the comparison of incident and diffracted energy is required is the directional energy flux represented by the Poynting vector $\boldsymbol{P} = \boldsymbol{E} \times \boldsymbol{H}^*$. Its magnitude $P = \sqrt{\boldsymbol{P} \cdot \boldsymbol{P}^*}$ indicates the density of the electromagnetic field power flux (in Wm^{-2}). The asterisk denotes the complex conjugate quantity.

If the incident beam has the assumed TM polarization, the Poynting vector can be expressed by components of intensity vectors $\boldsymbol{E}$ and $\boldsymbol{H}$

$$\boldsymbol{P} = (E_1, 0, E_3) \times (0, H_2^*, 0) = (-E_3 H_2^*, 0, E_1 H_2^*). \tag{6.1}$$

To illustrate this application we consider similar smooth sine interface S as in the previous chapter, but now we choose the profile height h comparable to the period Λ due to plasticity of presented results. In particular, $S\colon\ x_3 = \frac{1}{2}h(1 + \cos(2\pi x_1/\Lambda))$, $x_1 \in [0, \Lambda]$, $\Lambda = 500\,\mathrm{nm}$, $h = 200\,\mathrm{nm}$, separates glass superstrate ($n_1 = 1.5$) from gold substrate ($n_2 = 0.1838 + 3.43\mathrm{i}$). The incident beam of the red light ($\lambda = 632.8$ nm) again propagates under the incidence angle θ. Obtained values of the Poyntig vector magnitude are represented in Figure 5.

Presented theoretical model enables to specify an electromagnetic field distribution near spatially modulated dielectric/metal interface that is useful among other when surface plasmon polaritons are studied for sensoric applications.

7. Conclusion

The diffraction problem on a smooth interface between two homogeneous media was formulated as the system of boundary integral equations for the scalar factors of the electromagnetic intensities tangential fields. This formulation represents appropriate background of the numerical solution by the Boundary Elements Method (BEM). Obtained values of tangential fields enable to compute electromagnetic intensities on the boundary and above all to extrapolate these out of the boundary. The model functionality was verified for dielectrics as well as for absorbing materials. Presented results show possible applicability of the approach based on the tangential fields to such problems, where the detailed analysis of the diffracted optical field at an interface and/or in the near region is studied. A mathematical model for the diffraction on multi-layers is the future goal.

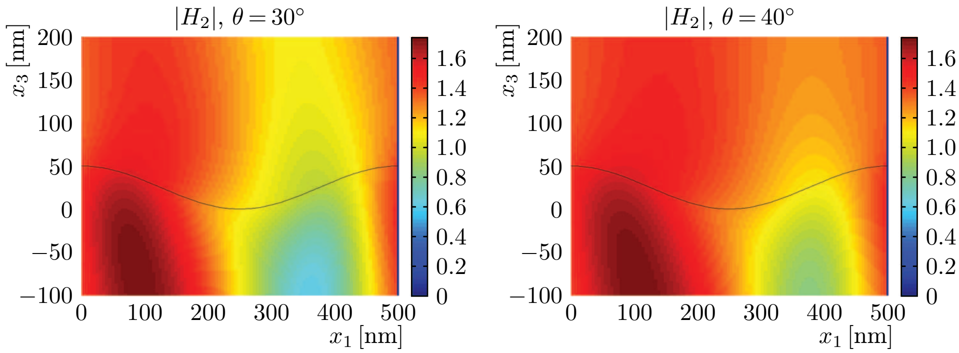

Figure 3. The $|H_2|$ component on air/glass interface for incidence angle θ.

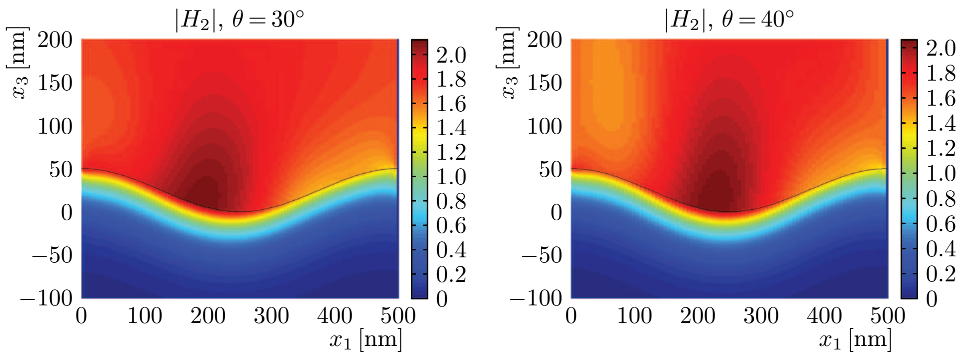

Figure 4. The $|H_2|$ component on glass/gold interface for incidence angle θ.

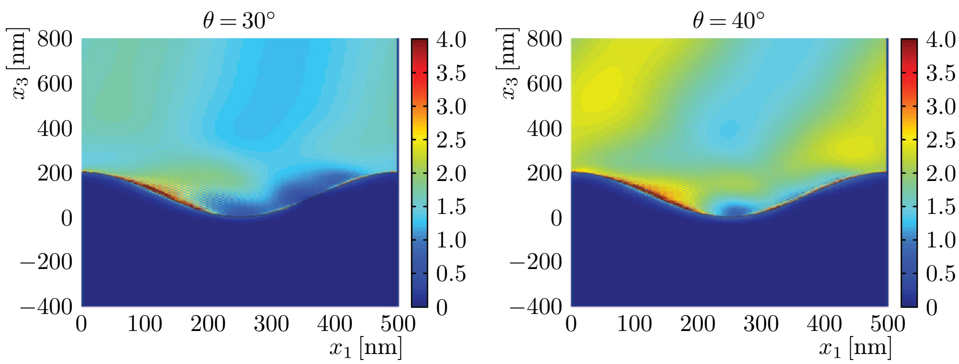

Figure 5. Poynting vector magnitude on glass/gold interface for incidence angle θ.

References

[1] *G. Bao, L. Cowsar, W. Masters* (eds.): Mathematicall Modelling in Optical Science. Frontiers in Applied Mathematics 22. SIAM, Philadelphia, 2001. zbl MR doi

[2] *M. Bonnet, M. Guiggiani*: Tangential derivative of singular boundary integrals with respect to the position of collocation points. Int. J. Numer. Methods Eng. *41* (1998), 1255–1275. zbl MR doi

[3] *A. Buffa, M. Costabel, C. Schwab*: Boundary element methods for Maxwell's equations on non-smooth domains. Numer. Math. *92* (2002), 679–710. zbl MR doi

[4] *A. Buffa, M. Costabel, D. Sheen*: On traces for $\mathbf{H}(\mathbf{curl}, \Omega)$ in Lipschitz domains. J. Math. Anal. Appl. *276* (2002), 845–867. zbl MR doi

[5] *S. N. Chandler-Wilde, A. T. Peplow*: A boundary integral equation formulation for the Helmholtz equation in a locally perturbed half-plane. ZAMM, Z. Angew. Math. Mech. *85* (2005), 79–88. zbl MR doi

[6] *X. Chen, A. Friedmann*: Maxwell's equations in a periodic structure. Trans. Am. Math. Soc. *323* (1991), 465–507. zbl MR doi

[7] *N. Chiu, S. Nien, C. Tu, J. Lee, C. Lin*: Advanced metal nanostructure design for surface plasmon photonic bandgap biosensor device. Annual International Conference of the IEEE Engineering in Medicine and Biology. IEEE, New York, 2006, pp. 6521–6524. doi

[8] *F. Flory, L. Escoubas, G. Berginc*: Optical properties of nanostructured materials: A review. J. Nanophotonics *5* (2011), Article ID 052502, 21 pages. doi

[9] *B. H. Kleemann, A. Mitreiter, F. Wyrowski*: Integral equation method with parametrization of grating profile theory and experiments. J. Modern Optics *43* (1996), 1323–1349. doi

[10] *J. Krček, J. Vlček, A. Žídek*: Tangential fields in optical diffraction problems. Programs and Algorithms of Numerical Mathematics 16. Academy of Sciences of the Czech Republic, Prague, 2013, pp. 124–129. zbl MR

[11] *L. Li*: Use of Fourier series in the analysis of discontinuous periodic structures. J. Optical Soc. Am., Ser. A *13* (1996), 1870–1876. doi

[12] *C. M. Linton*: The Green's function for the two-dimensional Helmholtz equation in periodic domains. J. Eng. Math. *33* (1998), 377–402. zbl MR doi

[13] *M. Nevière, E. Popov*: Light Propagation in Periodic Media: Differential Theory and Design. Marcel Dekker, New York, 2002. doi

[14] *O. Steinbach*: Numerical Approximation Methods for Elliptic Boundary Value Problems: Finite and Boundary Elements. Springer, New York, 2008. zbl MR doi

[15] *A. Taflove, S. Hagness, M. Piket-May*: Computational electrodynamics: The finite-difference time-domain method. The Electrical Engineering Handbook. Academic Press, Amsterdam, 2000, pp. 629–670. doi

[16] *A. Žídek, J. Vlček, J. Krček*: Solution of diffraction problems by boundary integral equations. Proceedings of APLIMAT 2012. Slovak University of Technology, Bratislava, 2012, pp. 221–229.

Author's address: *Jiří Krček*, Faculty of Mechanical Engineering, VSB—Technical University of Ostrava, 17. listopadu 2172/15, 708 00 Ostrava-Poruba, Czech Republic, e-mail: `jiri.krcek@vsb.cz`.